ORGANOMETALLICS

Article

Cite This: Organometallics 2020, 39, 388−396

pubs.acs.org/Organometallics

Synthesis and Reactivity of Re(III) and Re(V) Fischer Carbenes

Caleb A. Brown, Cassandra P. Lilly, Nikola S. Lambic, Roger D. Sommer, and Elon A. Ison*

Department of Chemistry, North Carolina State University, 2620 Yarbrough Drive, Raleigh, North Carolina 27695-8204, United States

Supporting Information

ABSTRACT: Direct insertion of CO and isocyanides, RNC, into Re−R bonds results in high-oxidation-state acyl and iminoacyl complexes that can be treated with an electrophile to generate rare examples of rhenium(III) and oxorhenium(V) Fischer carbenes. Experimental and computational studies suggest that, as expected, the carbene ligands are electrophilic at carbon. Further, an interesting correlation was observed between the ^{13}C NMR chemical shift and the natural charge at the carbene carbon, which suggests that the electrophilicity of the ligand can be tuned, with the substituent attached to the carbene carbon having the most influence.

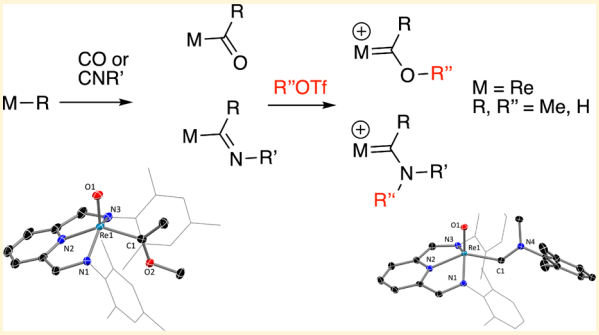

INTRODUCTION

Fischer carbenes are ubiquitous and usually contain transition metals in low oxidation states with π-acceptor ancillary ligands.[1−3] This is primarily because these complexes are usually accessible from low-valent metal carbonyl species that are treated with main-group organometallic reagents to yield acyl metalates, followed by treatment with an electrophilic reagent, as outlined in Scheme 1.[1]

Scheme 1. Synthetic Route to Fischer Carbene Complexes

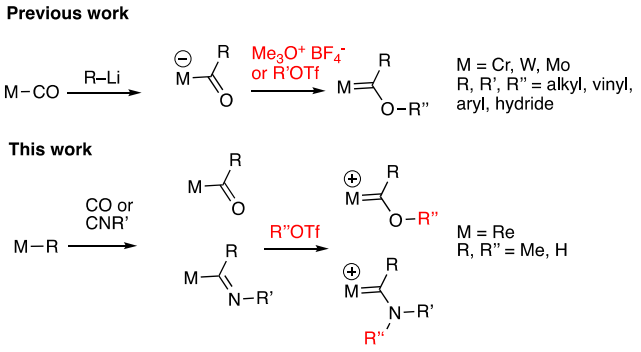

In contrast, Fischer carbene complexes with metals in high or intermediate oxidation states are quite rare, possibly because of the inability of metals to stabilize π-accepting carbonyl ligands.[4−6] Our group has recently described a unique mechanism for the generation of rhenium(V) acyl complexes that does not involve the prior formation of a carbonyl species but instead involves the direct insertion of CO into a Re−R (R = H, alkyl, aryl) bond.[7−10] In this paper we show that this strategy can be utilized to generate rare Re(III) and Re(V) Fischer carbene complexes.

RESULTS AND DISCUSSION

Synthesis of Re(III) and Re(V) Carbenes. The reaction of the complexes (O)Re(DAP)(C(O)CH_3) (DAP = 2,6-bis-((arylamino)methyl)pyridine; aryl = mesityl (**1a**) xylyl (**1b**)) with methyl triflate resulted in the formation of the cationic rhenium carbene complexes **2** (Scheme 2).

Scheme 2. Synthesis of Carbene Complexes 2

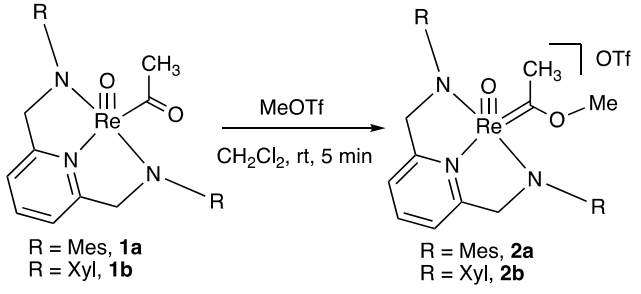

Slow diffusion of pentane into a concentrated solution of **2a** in dichloromethane led to X-ray-quality crystals that confirmed the addition of the methyl group to the acyl oxygen (Figure 1). The rhenium center is in an almost ideal square-pyramidal environment (τ = 0.06)[11] with a Re═C bond distance of 1.980(3) Å. This bond length is shorter than those of two other heteroatom-substituted oxorhenium carbene complexes reported in the literature. For example, the complex *fac*-[Re(O)Cl_3[CN(H)C_6H_4-2-O]$_2$]·$OPPh_3$[12] is reported to have a Re═C bond length of 2.095(4) Å, while this bond length is reported to be 2.080(5) Å for the complex [$ReOCl_2$(cbt)-(PPh_3)] (cbt = ((benzothiazol-2-ylamino)methylene)-

Received: September 1, 2019
Published: December 23, 2019

DOI: 10.1021/acs.organomet.9b00600
Organometallics 2020, 39, 388−396

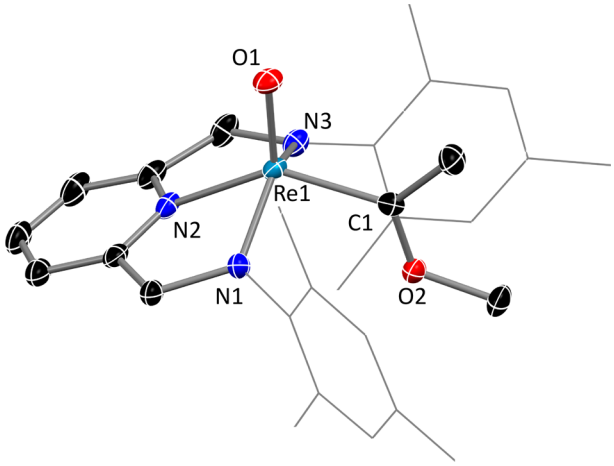

Figure 1. X-ray crystal structure of **2a**. Ellipsoids are at the 50% probability level. Hydrogen atoms and triflate counterion are omitted, and the mesityl substituents on the diamido ligand are depicted in wireframe for clarity. Selected bond lengths (Å) and bond angles (deg): Re1−O1, 1.695(2); Re1−N1, 1.957(3); Re1−N2, 2.063(3); Re−N3, 1.961(3); Re1−C1, 1.980(3); O2−C1, 1.302(4); O1−Re1−N3, 110.62(12); O1−Re1−N1, 111.76(12); N3−Re1−N1, 136.31(11); O1−Re1−N2, 115.91(13); N3−Re1−N2, 76.45(12); N1−Re1−N2, 76.09(11); O1−Re1−C1, 103.93(12); N3−Re1−C1, 90.26(12); N1−Re1−C1, 89.59(12); N2−Re1− C1, 140.17(11).

benzamide).[13] In addition, our group has reported that the complex [DAAmRe(O)(C(CH_3)OBF_3)] (DAAm = *N*,*N*-bis(2-arylaminoethyl)methylamine; aryl = C_6F_5) has a rhenium−carbene bond length of 2.0074(18) Å.[14]

In an analogous reaction, treatment of the Re(III) methyl complex (CO)Re(DAAm)(CH_3) (**3**) with alkyl and aryl isocyanide reagents followed by treatment with methyl triflate followed by H_2O results in the isolation of the Re(III) carbene complexes **5a,b** (Scheme 3). These reactions proceed by

Scheme 3. Synthesis of Re(III) Carbene Complexes

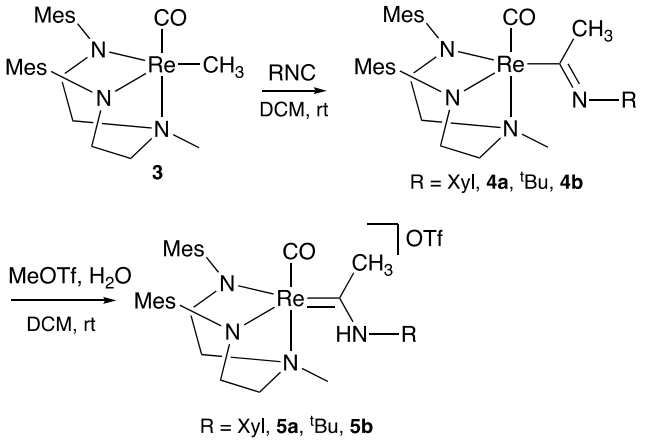

insertion of isocyanide into the Re−CH_3 bond to form iminoacyl complexes **4a** (R = Mes) and **4b** (R = Xyl). Complexes **4a,b** were not isolated but were identified by ^{1}H NMR spectroscopy (see the Supporting Information). These complexes were then converted quantitatively to complexes **5a,b**.

In previous work from our group we have shown that the oxorhenium hydride (O)ReDAP(H) (**6a**) is reduced with CO to produce the Re (I) tricarbonyl **7** (Scheme 4).[7] The proposed mechanism for this reaction involves insertion of CO into the Re−H bond.

Scheme 4. Mechanism for the Reductive Carbonylation of Rhenium Hydride 3

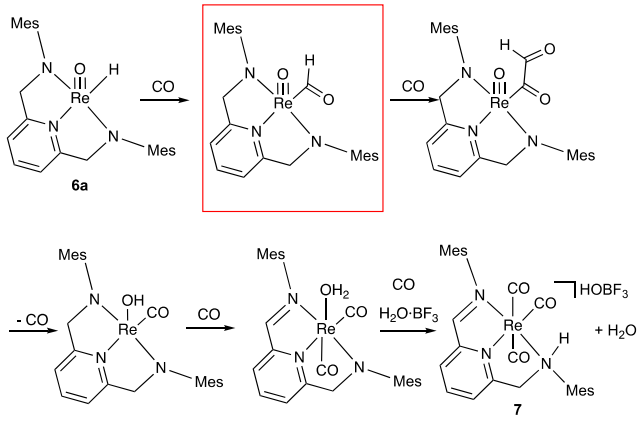

Given that isocyanides are isoelectronic with CO and in many cases exhibit similar reactivity, we explored the insertion of isocyanides into the Re−H bond. Thus, treatment of **6** (R = Mes (**6a**) Xyl (**6b**)) with XylNC, followed by methyl triflate (MeOTf), results in the isolation of the oxorhenium carbene complexes **8a** (R = Mes) and **8b** (R = Xyl) (Scheme 5).

Scheme 5. Re(V) Carbenes from the Insertion of Isocyanides into Re−H Bonds

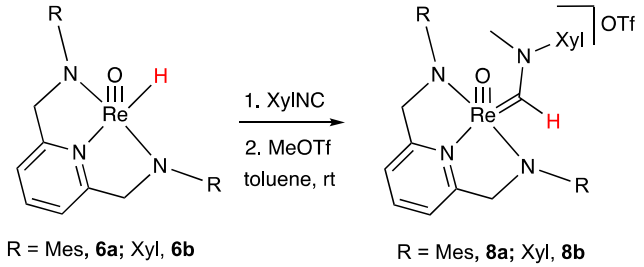

Complexes **8** are rare examples of carbenes featuring an oxo ligand and a heterosubstituted carbene ligand. Other examples include the neutral complex Tp′W(O)(I)(=C(R)OR′) (Tp′ = hydridotris(3,5-dimethylpyrazolyl)borate; R = Me, Ph; R′ = H, $SiPh_2Me$) and the cationic hydroxy carbene complex [Tp′W(O)(NCMe)(=C(Me)OH)]$^+$, reported by the Templeton group.[4] In addition, W[C(Ph)$C_3H_3N_2BHPz_2$)](O)(Br_2) was reported by Mayr and co-workers.[15] Examples of actinide[16] complexes with N-heterocyclic carbenes (NHCs) have also been reported.

X-ray-quality crystals of **8b** were obtained by the slow diffusion of pentane into a methylene chloride solution of the complex (Figure 2). The rhenium atom is in an almost ideal square-pyramidal environment (τ = 0.09)[11] with the Re−C(carbene) bond (Re1−C1, 2.021(2) Å) within range (1.85−2.205 Å) for a rhenium carbene.

Analogously to Scheme 3, the reaction presumably proceeds by insertion of XylNC into a Re−R (R = H) bond to form an iminoformyl group, which reacts with a Lewis acid (MeOTf) to generate the carbene complex. This type of reactivity is also observed in the reaction of $B(C_6F_5)_3/H_2O$ with **6** (Scheme 6). In the ^{1}H NMR spectrum for the product **10a**, two doublets at

DOI: 10.1021/acs.organomet.9b00600
Organometallics 2020, 39, 388−396

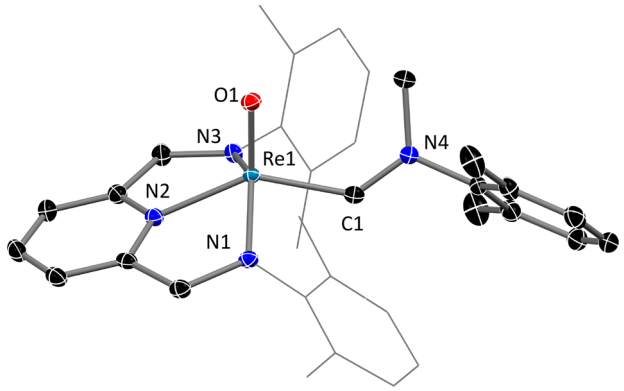

Figure 2. X-ray crystal structure of **8b**. Thermal ellipsoids are at the 50% probability level. Hydrogen atoms and triflate counterion are omitted, and the xylyl substituents on the diamido ligand are depicted in wireframe for clarity. Selected bond lengths (Å) and angles (deg): Re1−O1, 1.689(2); Re1−C1, 2.021(2); Re1−N2, 2.058(1); Re1−N3, 1.968(1); Re1−N1, 1.961(2); C1−N4, 1.311(2); Re1−C1−N4, 131.4(1).

Scheme 6. Re(V) Carbenes from the Insertion of Isocyanides into Re−H Bonds in the Presence of $B(C_6F_5)_3/H_2O$

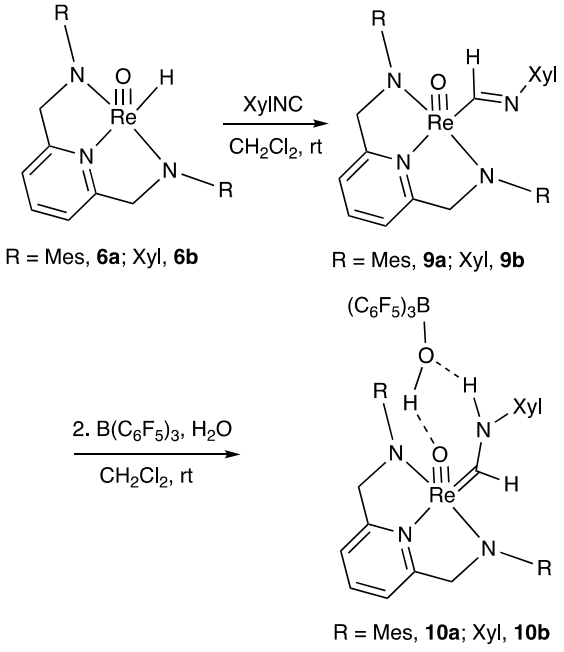

9.7 and 13.5 ppm (J = 16.4 Hz) are observed. The magnitude of the coupling constant is indicative of C−H/N−H coupling.

X-ray-quality crystals were obtained from the diffusion of pentane into a concentrated solution of **10a** in dichloromethane (Figure 3). The X-ray structure shows a cationic oxorhenium complex with a hydroxyborate ($HOB(C_6F_5)_3$) anion. This is consistent with the observations by ^{1}H NMR spectroscopy.

The rhenium atom in **10a** is in a distorted-square-pyramidal environment (τ = 0.16)[11] with the oxo ligand in the apical position. The Re−C(carbene) bond length is relatively short. It is similar in length to those in Re acyl complexes previously isolated by the Ison group, where the Re−C(acyl) bond was 2.026−2.028 Å.[17−19] The formation of the hydroxyborate anion $HOB(C_6F_5)_3$ likely proceeds via the reaction of $B(C_6F_5)_3$ with H_2O to form the Brønsted acid $H_2O{\cdot}B(C_6F_5)_3$, which protonates the iminoformyl intermediate **9a** to form the cationic

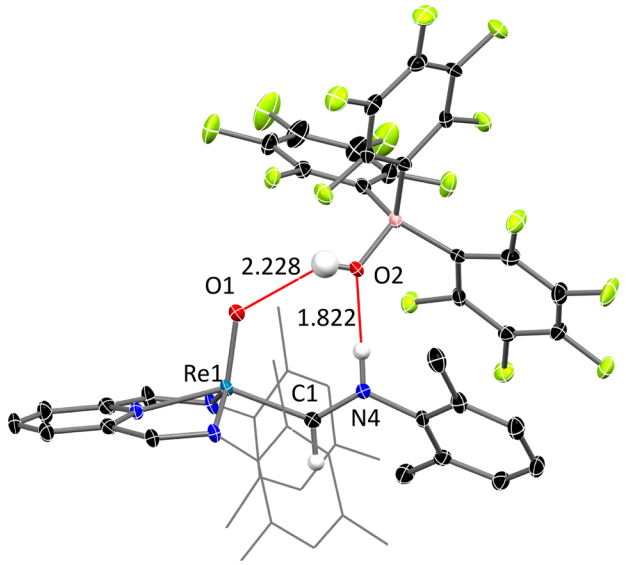

Figure 3. X-ray crystal structure of **10a**. Thermal ellipsoids are at the 50% probability level. Selected hydrogen atoms are shown, and the mesityl substituents on the diamido ligand are depicted in wireframe for clarity. Hydrogen-bonding contacts (Å) are shown in red. Selected bond lengths (Å) and angles (deg): Re1−O1, 1.6877(17); Re1−C1, 2.029(3); B1−O2, 1.479(3); C1−N4, 1.298(3); Re1−C1−N4, 129.48(19); O1−Re1−C1, 102.82(9).

carbene and hydroxyborate anion. Adducts such as $H_2O{\cdot}B(C_6F_5)_3$ are well-known and have been shown to be strong Brønsted acids with a pK_a value of 8.4 in acetonitrile and a hypothetical aqueous pK_a value of less than 0.9.[20]

To test the hypothesis that $H_2O{\cdot}B(C_6F_5)_3$ is involved as the Brønsted acid, the reaction with rigorously dried solvent and reagents was examined. In contrast to the reaction described in Scheme 6, the solution briefly turned green before turning bright purple. Additionally, the doublet corresponding to the protonated complex **10a** was not observed. Instead, a singlet was observed at approximately 9.22 ppm (tentatively assigned as the iminoformyl intermediate **9a**). Upon titration with water, the singlet decayed and the doublet attributed to **10a** was observed (see the Supporting Information). This experiment suggests that the iminoformyl intermediate **9a** was generated initially, which was subsequently protonated to give the final carbene salt **10a**. Attempts to isolate **9a** were unsuccessful.

To summarize, the strategy of CO and CNR insertion into Re−R (R = CH_3, H) bonds was utilized to generate Re(III) and Re(V) carbenes. The method is quite general and does not require prior formation of stable Re−CO adducts, thus allowing for the accessibility of carbenes with rhenium in medium to high oxidation states. The synthesis of these complexes allowed for an examination of their reactivity.

Reactivity of Re(III) and Re(V) Carbenes. The insertion reaction of the oxorhenium(V) hydride **6a** with isocyanides in the absence of $B(C_6F_5)_3$ was examined (Scheme 7). Unlike the corresponding reaction in the presence of the Lewis acid, several diastereotopic peaks from the ligand are observed by ^{1}H NMR spectroscopy, which suggests that there are several rhenium species present. After the reaction mixture was allowed to stand for 2 days, a single rhenium species was observed by ^{1}H NMR spectroscopy. This species was not the cationic carbene complex as described previously; instead, complex **14** was isolated as well as the organic product 2,6-dimethylaniline (Scheme 7).

DOI: 10.1021/acs.organomet.9b00600
Organometallics 2020, 39, 388−396

Scheme 7. Insertion of XylNC in the Absence of Lewis Acid

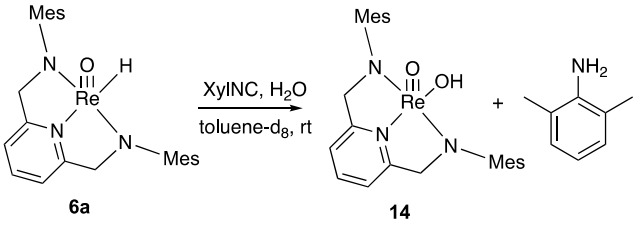

X-ray-quality crystals were obtained by diffusion of pentane into a concentrated dichloromethane solution of **14** (Figure 4).

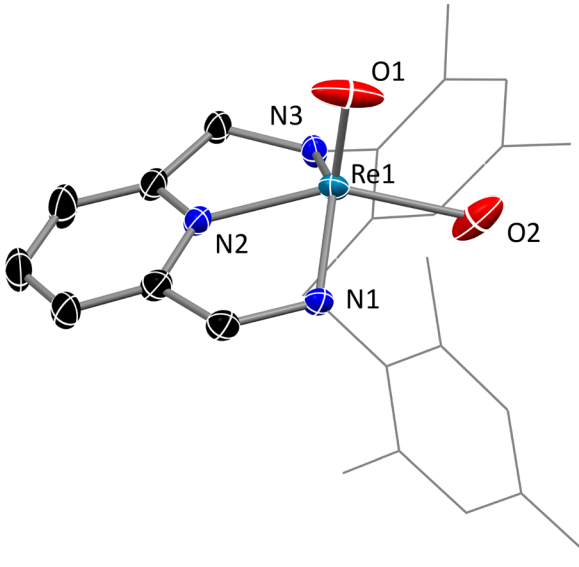

Figure 4. X-ray crystal structure of **14**. Thermal ellipsoids are at the 50% probability level. The aryl rings of the ancillary ligand are shown in wireframe for clarity. Selected bond lengths (Å) and angles (deg): Re1−O1, 1.681(6); Re1−O2, 2.121(7); Re1−N1, 1.968(5); Re1−N2, 2.057(6); Re1−N3, 1.965(5); O1−Re1−O2, 96.1(4); O1−Re1−N1, 112.0(3); O1−Re1−N2, 115.5(4); O1−Re1−N3, 111.8(3).

In **14**, rhenium is in a distorted-square-pyramidal environment ($\tau = 0.23$)[11] with the oxo ligand in the apical position. The Re−oxo bond length is consistent with those in other DAP oxorhenium(V) complexes.[17,18,21,22]

The reactivity described above is consistent with isocyanide insertion into a Re−R (R = alkyl, hydride) bond to form an iminoformyl or an iminoacyl intermediate, followed by protonation with a Brønsted acid to form a Fischer carbene. The addition of water to solutions of MeOTf or $B(C_6F_5)_3$ lowers the pK_a in solution by the release of H^+. The observed reactivity in the absence of a Lewis acid is consistent with the electrophilic reactivity of Fischer carbenes, which are known to react with nucleophiles at the carbene carbon to undergo exchange reactions via tetrahedral intermediates.[23] Given this precedent, a proposed mechanism for the formation of **14** is shown in Scheme 8 where the Fischer carbene **10a^{OH}** reacts via the tetrahedral (at carbon) intermediate **11** to produce the carbene **13**. The viability of this mechanism was also supported by a detailed computational study (see the Supporting Information).

Electronic Structure of Carbene Complexes. The reactivity described above suggests that the carbene ligands are electrophilic at carbon and thus should be regarded as Fischer type carbenes. However, there is some ambiguity, as the

Scheme 8. Proposed Mechanism for the Formation of 14

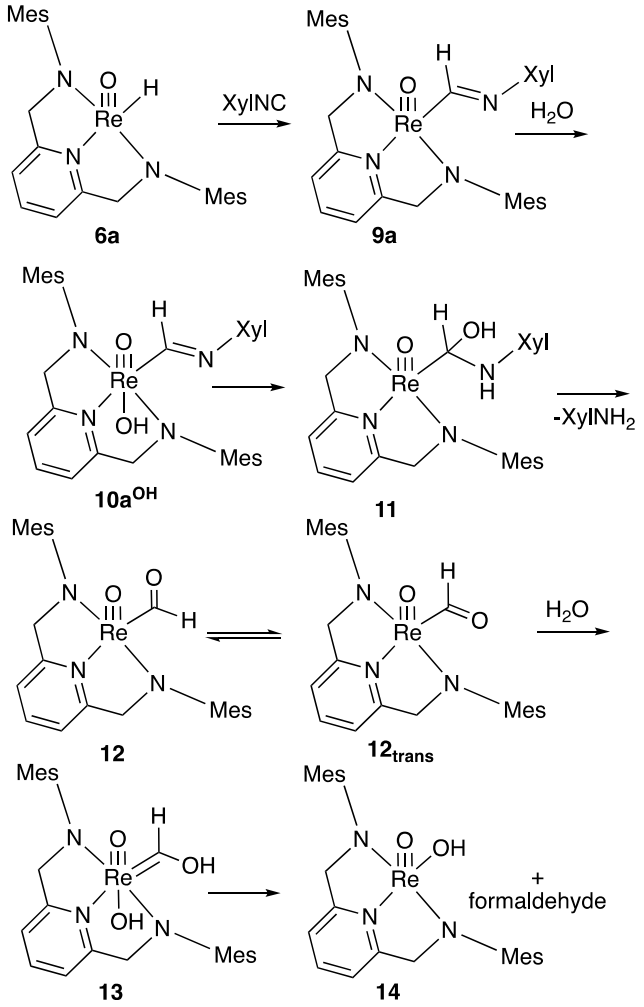

ligands may be regarded as $CR(OR)^{2-}$ ligands and thus the metal complexes can be viewed as d^0 Re(VII) and d^2 Re(V), respectively. To address this ambiguity, we performed a series of density functional theory (DFT) calculations to examine the bonding of the carbene ligand in these complexes. On the basis of previous benchmarking for oxorhenium complexes,[14,17−19,24] calculations were carried out the DFT (B3PW91+D3)[25−26] level of theory. The complexes calculated in this aspect of the study are depicted in Chart 1.

The bonding in Fischer carbenes is often described as synergistic: i.e., resulting from simultaneous σ donation from the carbene ligand and π back-bonding from the metal to the LUMO of the carbene.[23] Inspection of the natural bonding orbitals (NBOs)[27,28] for **2b**, a typical oxorhenium carbene, shows clearly σ-bonding and -antibonding combinations between the rhenium atom and the carbene ligand (Figure 5a,b) and the π-bonding and -antibonding combination between the rhenium d_{xy} orbital and the π^* orbital from the carbene ligand (Figure 5c,d).

To further quantify the extent of σ donation and π back-bonding, a fragment orbital analysis was applied using the AOMix 6.0 program.[29,30] As shown in Table 1, for all complexes studied the σ donation from the carbene ligand is more extensive than π back-bonding. This is consistent with the viewpoint that the Fischer carbenes examined here are electrophilic at carbon.

DOI: 10.1021/acs.organomet.9b00600
Organometallics 2020, 39, 388−396

Chart 1. Calculated Carbene Complexes

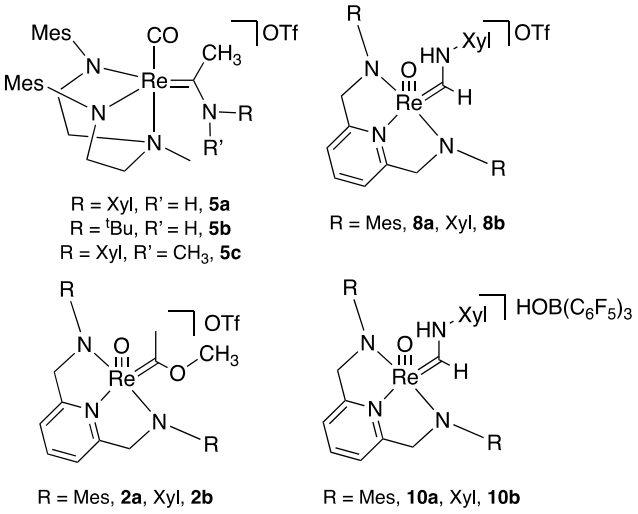

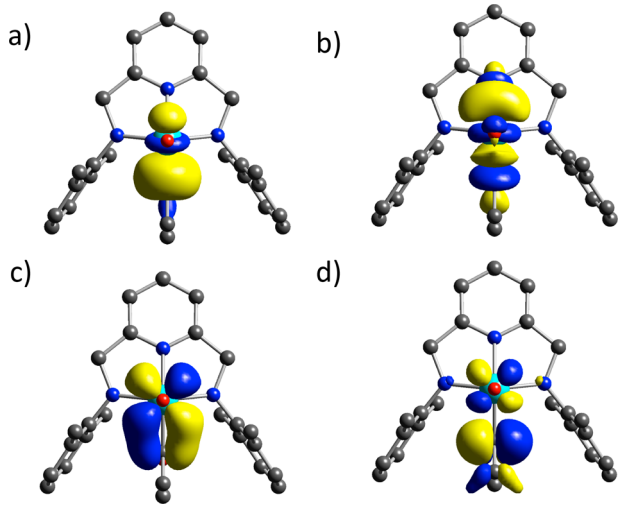

Figure 5. Natural bonding orbitals for **2b** showing (a, b) σ-bonding and -antibonding combinations between rhenium and the carbene ligand and (c, d) π-bonding and -antibonding combinations between the carbene ligand and a d_{xy} orbital. NBO analysis: (a) orbital 48 (bonding), occupancy 1.88, 33% rhenium, 67% carbon; (b) orbital 125 (antibonding), occupancy 0.21, 67% rhenium, 33% carbon; (c) orbital 30 (lone pair Re), occupancy 1.65, 99% rhenium d orbital; (d) orbital 120 (lone pair vacancy C), occupancy 0.66, 99% carbon p orbital.

Table 1. Charge Decomposition Analysis (CDA)[a] of Bonding in Re(III) and Re(V) Carbenes

entry	complex	σ donation	π back-bonding	net charge donation
1	**5a**	0.213	0.107	0.303
2	**5b**	0.216	0.113	0.290
3	**7a**	0.247	0.145	0.315
4	**7b**	0.244	0.140	0.321
5	**2a**	0.228	0.130	0.255
6	**2b**	0.230	0.128	0.258
7	**10a**	0.227	0.138	0.297
8	**10b**	0.221	0.132	0.298

[a]CDA analysis was performed with the AOMix 6.0 software program. See Computational Methods for details.

To explore the electrophilicity further, we examined the NBO partial charge at the carbene carbon in addition to the calculated ^{13}C NMR shifts as implemented in Gaussian 09.[31] It was observed experimentally that the carbene carbons in complexes **2**, **5**, **8**, and **10** are significantly deshielded and occur from ~240 to 300 ppm in the ^{13}C NMR spectrum. Chemical shifts for complexes **2**, **5**, **8**, and **10** were calculated, and as shown in Figure 6a, there is good agreement with the experimental values (R^2 = 0.92).

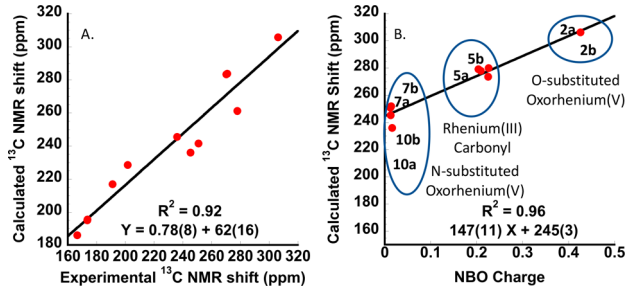

Figure 6. (A) Correlation between calculated and experimental ^{13}C NMR shifts. (B) Correlation between the calculated ^{13}C NMR shift and the natural charge. Calculations were performed at the B3PW91-D3/6-311G++(d,p)[34,35] level utilizing the gauge-independent atomic orbital (GIAO) method[36−40] and are referenced to TMS.

As shown in Figure 6b, there is a strong correlation between the calculated ^{13}C NMR shift and the NBO charge. Further, the charge at carbon appears to be most dramatically affected by the substituent on the carbene carbon, with O-substituted ligands observed with higher chemical shifts (more deshielded) and more positive natural charges in comparison to the corresponding complexes with N substituents.[32,33] Also interesting from the data is the influence of formal oxidation state, as the rhenium carbonyl complexes (formally Re(III)) have carbene carbons with chemical shifts and NBO charges intermediate between N-substituted and O-substituted oxorhenium carbenes (formally Re(V)), suggesting that the formal oxidation state has a smaller influence than the substituent on the carbene carbon.

■ CONCLUSIONS

Direct insertion of CO and isocyanides (CNR) into Re−R bonds result in high-oxidation-state acyl and iminoacyl complexes that can be treated with an electrophile to generate rare examples of Re(III) and (O)Re(V) Fischer carbenes. This strategy is different from the classic Fischer carbene synthesis, which relies on nucleophilic addition to a carbonyl ligand in a neutral metal complex, followed by the treatment of this anionic acyl metalate with an electrophile. Experimental and computational studies suggest that, as expected, the carbene ligands are electrophilic at carbon. Further, an interesting correlation was observed between the ^{13}C NMR chemical shift and the natural charge at the carbene carbon, which suggests that the electrophilicity of the ligand can be tuned, with the substituent attached to carbene carbon having the most influence.

■ EXPERIMENTAL SECTION

General Considerations. DAP (DAP = 2,6-bis((arylamino)-methyl)pyridine; aryl = xylyl)[41] and $(SMe_2)Re(O)Cl_3(OPPh_3)$,[42] were prepared as reported in the literature. All reactions were conducted under nitrogen in a glovebox or using standard Schlenk line techniques unless otherwise noted. All other reagents were purchased from commercial sources and used as received. ^{1}H, ^{13}C, and ^{19}F NMR spectra were obtained on a Varian Mercury 400 MHz, a Varian Mercury 300 MHz, or a Brüker 500 or 700 MHz spectrometer at

DOI: 10.1021/acs.organomet.9b00600
Organometallics 2020, 39, 388−396

room temperature. Chemical shifts are given in parts per million (ppm) and are referenced to the residual protons or carbons of the deuterated solvents, respectively. Elemental analyses were performed by Atlantic Microlabs, Inc. X-ray crystallography was performed at the X-ray Structural Facility of North Carolina State University.

(O)Re(DAP)Cl (DAP = 2,6-Bis((arylamino)methyl)pyridine; Aryl = Xylyl). $(SMe_2)Re(O)Cl_3(OPPh_3)$ (450 mg, 0.69 mmol) and DAP (DAP = 2,6-Bis((arylamino)methyl)pyridine; aryl = xylyl (450 mg, 1.30 mmol) were dissolved in EtOH. 2,6-Lutidine (0.8 mL, 6.9 mmol) was then added, and the reaction mixture was stirred overnight. The reaction was then vacuum filtered and dried. The complex was obtained as a green solid (256 mg) in 64% yield. ^{1}H NMR (CD_2Cl_2, 300 MHz): δ 8.24 (t, J = 7.6 Hz, 1H, pyr-*para* H) 7.88 (d, J = 7.6 Hz, 2H, pyr-*meta* H) 7.14−6.96 (overlapping m, 6H, XyDAP-aryl H) 5.69 (d, J = 20.5 Hz, 2H, pyr-CH_2-N) 5.52 (d, J = 20.5 Hz, 2H, pyr-CH_2-N) 2.51 (s, 6H, XyDAP-CH_3) 1.66 (s, 6H, XyDAP-CH_3). ^{13}C NMR (CD_2Cl_2, 176 MHz): δ 167.80, 156.79, 143.40, 136.31, 135.11, 127.92, 127.75, 125.21, 125.19, 117.11, 79.38, 18.10, 17.94. Anal. Calcd: C, 47.54; N, 7.23; H, 4.34. Found: C, 47.19; N, 7.16; H, 4.43.

(O)Re(DAP)CH_3 (DAP = 2,6-Bis((arylamino)methyl)pyridine; Aryl = Xylyl). (O)Re(DAP)Cl (332.0 mg, 0.512 mmol) was dissolved in CH_2Cl_2. Methylmagnesium bromide (3.0 M in diethyl ether) (0.34 mL, 1.02 mmol) was added via syringe. The reaction mixture was then stirred for 24 h. The reaction mixture was then removed from the glovebox and quenched dropwise with water. The resulting mixture was extracted with CH_2Cl_2 three times and dried over Na_2SO_4. The solvent was then removed in vacuo. The complex was obtained as a dark purple solid (247 mg) in 86% yield. ^{1}H NMR (300 MHz, CD_2Cl_2): δ 8.08 (t, J = 7.8 Hz, 1H, pyr-*para*-H), 7.71 (d, J = 7.8 Hz, 2H, pyr-*meta*-H), 7.15 (d, J = 7.5 Hz, 2H, XyDAP-*meta*-H), 7.08 (d, J = 7.4 Hz, 2H, XyDAP-*meta*-H), 6.97 (t, J = 7.4 Hz, 1H, XyDAP-*para*-H), 5.67 (d, J = 20.1 Hz, 2H, pyr-CH_2-N), 5.47 (d, J = 20.1 Hz, 2H, pyr-CH_2-N), 2.44 (s, 6H, XyDAP-CH_3), 1.75 (s, 3H, Re-CH_3), 1.58 (s, 6H, XyDAP-CH_3). ^{13}C NMR (151 MHz, CD_2Cl_2): δ 168.09, 155.72, 140.96, 136.89, 135.06, 127.97, 127.80, 126.86, 124.50, 116.23, 78.73, 18.12, 17.46, 13.72. Anal. Calcd: C, 51.41; N, 7.49; H, 5.03. Found: C, 51.41; N, 7.67; H, 5.02.

(O)Re(DAP)C(O)CH_3 (DAP = 2,6-Bis((arylamino)methyl)-pyridine; Aryl = Xylyl; 1b). **1b** was synthesized according to the literature procedure.[17] ^{1}H NMR (Benzene-d_6, 700 MHz): δ 7.07 (m, 4H, XyDAP-*meta*-H), 6.96 (t, J = 7.5 Hz, 2H, XyDAP-*para*-H), 6.78 (t, J = 7.8 Hz, 1H, pyr-*para*-H), 6.35 (d, J = 7.8 Hz, 2H, pyr-*meta*-H), 5.04 (d, J = 20.5 Hz, 2H, pyr-CH_2-N), 4.88 (d, J = 20.5 Hz, 2H, pyr-CH_2-N), 2.76 (s, 6H, xyDAP-CH_3), 2.11 (s, 3H, acyl-CH_3), 2.05 (s, 6H, xyDAP-CH_3). ^{13}C NMR (Benzene-d_6, 176 MHz): δ 255.88, 166.93, 156.14, 139.46, 136.31, 135.77, 132.08, 131.33, 125.22, 115.97, 74.45, 47.26, 18.54, 18.40. Complex **1b** is a precursor to **2b** and was used without further purification.

[(DAP)Re(O)(CC(CH_3)OCH_3)][OTf] (DAP = 2,6-Bis-((arylamino)methyl)pyridine; Aryl = Mesityl; 2a). Methyl triflate (0.486 mmol, 53.4 μL) was added to a concentrated solution of **1a** (0.486 mmol, 300 mg) in dichloromethane. Excess hexanes was added to precipitate the product. The dark red powder was filtered and isolated in a 78% yield. ^{1}H NMR (CD_2Cl_2, 600 MHz): δ 8.38 (t, J = 7.9 Hz, 1H, pyr-*para*-H), 7.87 (d, J = 7.9 Hz, 2H, pyr-*meta*-H), 6.86 (s, 2H, MesDAP-*meta*-H), 6.79 (s, 2H, MesDAP-*meta*-H), 5.93 (d, J = 20.6 Hz, 2H, pyr-CH_2-N), 5.56 (d, J = 20.7 Hz, 2H, pyr-CH_2-N), 3.27 (s, 3H, O-CH_3), 2.61 (s, 3H, carbene-CH_3), 2.44 (s, 6H, MesDAP-CH_3), 2.21 (s, 6H, MesDAP-CH_3), 1.85 (s, 6H, MesDAP-CH_3). ^{13}C NMR (176 MHz, CD_2Cl_2): δ 304.59, 164.94, 152.11, 144.36, 136.78, 134.79, 133.34, 129.54, 128.31, 119.73, 72.67, 61.69, 36.76, 20.42, 17.83, 17.31. Anal. Calcd: C, 44.61; N, 5.38; H, 4.52. Found: C, 44.94; N, 4.97; H, 4.85.

[(DAP)Re(O)(C(CH_3)OCH_3)]][OTf] (DAP = 2,6-Bis((arylamino)-methyl)pyridine; Aryl = Xylyl; 2b). Methyl triflate (0.087 mmol, 9.6 μL) was added to a concentrated solution of **1b** (0.087 mmol, 54 mg) in dichloromethane. Excess hexanes were added to precipitate the product. The dark red powder was filtered and isolated in a The complex was obtained as a dark purple solid in 83% yield. ^{1}H NMR (CD_2Cl_2, 500 MHz): δ 8.40 (t, J = 7.9 Hz, 1H, pyr-*para*-H), 7.91 (d, J = 7.9 Hz, 2H, pyr-*meta*-H), 7.06 (d, J = 7.6 Hz, 2H, XyDAP-*meta*-H), 6.98 (d, J = 7.5 Hz, 2H, XyDAP-*meta*-H), 6.90 (t, J = 7.5 Hz, 2H, XyDAP-*para*-H), 5.97 (d, J = 20.8 Hz, 2H, pyr-CH_2-N), 5.61 (d, J = 20.8 Hz, 2H, pyr- CH_2-N), 3.24 (s, 3H, O-CH_3), 2.58 (s, 3H, Carbene-CH_3), 2.48 (s, 6H, XyDAP-CH_3), 1.90 (s, 6H, XyDAPCH_3). ^{13}C NMR (CD_2Cl_2, 151 MHz): δ 304.86, 164.90, 154.39, 144.61, 135.15, 133.83, 129.05, 127.79, 127.07, 119.96, 72.45, 61.83, 36.85, 17.89, 17.38. Attempts to purify this compound for elemental analysis resulted in the formation of an oil.

DAAmRe(CO)CH_3 (DAAm = N^1-Mesityl-N^2-(2-(mesitylamino)-ethyl)-N^2-methylethane-1,2-diamine; 3). DAAmRe(CO)(OAc) (653 mg, 1.04 mmol) was dissolved in CH_2Cl_2. Five equivalents of MeMgBr (3.0 M in diethyl ether) (1.74 mL, 5.20 mmol) was added via syringe. The reaction mixture was then stirred overnight. The reaction mixture was then removed from the glovebox and quenched dropwise with water. The resulting mixture was extracted with CH_2Cl_2 three times and dried over Na_2SO_4. The solvent was then removed in vacuo. The complex was obtained as a reddish orange solid in 90% yield. ^{1}H NMR (500 MHz, CD_2Cl_2): δ 6.74 (m, 4H, overlapping MesDAP *meta*-H), 3.56 (m, 2H, MesDAAm −CH_2−), 3.45−3.37 (m, 2H, MesDAAm −CH_2−), 3.09−3.02 (m, 2H, MesDAAm −CH_2−), 2.93−2.86 (m, 5H, overlapping MesDAAm −CH_2− and N-CH_3), 2.19 (s, 6H Mes-CH_3), 2.11 (s, 6H, Mes-CH_3), 1.90 (s, 6H, Mes-CH_3), 1.37 (s, 3H, Re-CH_3). ^{13}C NMR (176 MHz, CD_2Cl_2): δ 202.13, 157.66, 133.75, 132.27, 130.16, 128.56, 128.33, 61.03, 58.84, 45.04, 20.34, 18.80, 14.45. Anal. Calcd for $C_{25}H_{36}N_3ORe\cdot 1/4CH_2Cl_2$: C, 50.38; N, 6.98; H, 6.11. Found: C, 50.71; N, 7.17; H, 5.98.

[DAAmRe(CO)(C(CH_3)NHC(CH_3)$_3$)][OTf] (DAAm = N^1-Mesityl-N^2-(2-(mesitylamino)ethyl)-N^2-methylethane-1,2-diamine; 5b). Complex **3** (188 mg, 0.324 mmol) was dissolved in CH_2Cl_2. One equivalent of *tert*-butyl isocyanide (36.6 μL, 0.324 mmol) was added via a microsyringe. Methyl trifluoromethanesulfonate (36.6 μL, 0.324 mmol) was added via a microsyringe to the reaction mixture. The reaction mixture was stirred for 1 h, and then water (50 μL) was added via syringe. The reaction mixture was stirred overnight. Brine was added to the reaction mixture, and the resulting mixture was extracted three times with CH_2Cl_2 and dried over Na_2SO_4. The solvent was then removed in vacuo to give the complex as a dark orange powder. ^{1}H NMR (700 MHz, CD_2Cl_2): δ 8.71 (s, 1H, Carbene-NH), 6.97 (s, 2H, MesDAAm *meta*-H), 6.90 (s, 2H, MesDAAm *meta*-H), 4.09 (m, 2H, MesDAAm -CH_2-), 3.83 (m, 2H, MesDAAm -CH_2-), 3.34 (m, 2H, , MesDAAm -CH_2), 3.27 (m, 2H, MesDAAm -CH_2-), 3.16 (s, 3H, MesDAAm N-CH_3), 2.53 (s, 3H, Carbene C-CH_3), 2.36 (m, 12H, overlapping MesDAAm-CH_3), 2.06 (s, 3H, MesDAAm-CH_3), 1.60 (s, 9H, Carbene *tert*-butyl), 1.58 (s, 3H, MesDAAm-CH_3). ^{13}C NMR (176 MHz, CD_2Cl_2): δ 261.31, 198.56, 156.22, 129.97, 129.51, 129.45, 63.62, 58.90, 49.51, 30.05, 24.80, 20.27, 19.49. Anal. Calcd for $C_{31}H_{46}F_3N_4O_4ReS\cdot 1/3C_5H_{12}$: C, 46.82; N, 6.69; H, 6.01. Found: C, 46.64; N, 6.52; H, 6.24.

(O)Re(DAP)H (DAP = 2,6-Bis((arylamino)methyl)pyridine; Aryl = Xylyl; 6b). (O)Re(DAP)Cl (332.0 mg, 0.512 mmol) was dissolved in THF. Tributyltin hydride (0.9 mL, 3.35 mmol) was added via syringe. The reaction mixture was then stirred for 24 h. The reaction mixture was then removed from the glovebox and solvent was removed in vacuo. The residue was then dissolved in minimal dichloromethane then crashed out with excess pentane before being isolated by vacuum filtration. The complex was obtained as a dark red solid in 87% yield. ^{1}H NMR (CD_2Cl_2, 300 MHz): δ 8.09 (t, J = 7.6 Hz, 1H, pyr-*para* H), 7.71 (d, J = 7.6 Hz, 2H, pyr-*meta* H), 7.07 (d, J = 7.6 Hz, 2H, XyDAP-*meta* H), 7.0 (d, J = 7.6 Hz, 2H, XyDAP-*meta* H), 6.88 (t, J = 7.6 Hz, 2H, XyDAP-*para* H), 6.06 (s, 1H, Re−H), 5.69 (d, J = 20.5 Hz, 2H, pyr-CH_2-N), 5.46 (d, J = 20.5 Hz, 2H, pyr-CH_2-N), 2.49 (s, 6H, XyDAP-CH_3), 1.77 (s, 6H, XyDAP-CH_3). ^{13}C NMR (CD_2Cl_2, 151 MHz): δ 168.94, 161.48, 141.16, 135.82, 133.36, 127.99, 127.91, 124.43, 116.54, 77.38, 18.33, 17.93. Anal. Calcd for $C_{23}H_{26}N_3ORe\cdot 1/3CH_2Cl_2$: C, 48.74; N, 7.31; H, 4.67. Found: C, 48.88; N, 7.26; H, 4.78.

(XyDAP)Re(O)D (6b-D). (O)Re(DAP)Cl (320.0 mg, 0.516 mmol) was dissolved in THF. Tributyltin deuteride (0.74 mL, 2.75 mmol) was added via syringe. The reaction mixture was then stirred for 24 h. The reaction mixture was then removed from the glovebox, and solvent was removed in vacuo. The residue was then dissolved in minimal

DOI: 10.1021/acs.organomet.9b00600
Organometallics 2020, 39, 388−396

dichloromethane and then crashed out with excess pentane before being isolated by vacuum filtration. The complex was obtained as a dark red solid in 81% yield. ^{1}H NMR (CD_2Cl_2, 300 MHz): δ 8.09 (t, J = 7.6 Hz, 1H, pyr-*para* H), 7.71 (d, J = 7.6 Hz, 2H, pyr-*meta* H), 7.07 (d, J = 7.6 Hz, 2H, XyDAP-*meta* H), 7.0 (d, J = 7.6 Hz, 2H, XyDAP-*meta* H), 6.88 (t, J = 7.6 Hz, 2H, XyDAP-*para* H), 5.69 (d, J = 20.5 Hz, 2H, pyr-CH_2-N), 5.46 (d, J = 20.5 Hz, 2H, pyr-CH_2-N), 2.49 (s, 6H, XyDAP-CH_3), 1.77 (s, 6H, XyDAP-CH_3).

[(O)Re(DAP)(CHN(CH$_3$)(2,6-(CH$_3$)$_2$C$_6$H$_3$))][OTf] (DAP = 2,6-Bis((arylamino)methyl)pyridine; Aryl = Mesityl; 8a). Complex **6a** (155 mg, 0.087 mmol) was dissolved in dichloromethane. 2,6-Dimethylphenyl isocyanide (22.8 mg, 0.174 mmol) was then added, and the reaction mixture was stirred for 5 min. Solvent was then removed in vacuo, and the resulting residue was washed with hexane, which was then removed via cannula filtration. The residue was then dissolved in dichloromethane, methyl trifluoromethanesulfonate (19.7 μL, 0.174 mmol) was then added via syringe, and the reaction mixture was stirred for an additional 15 min. The solvent was then removed in vacuo, and the resulting residue was dissolved in minimal dichloromethane and precipitated with excess pentanes to give the complex in 27% yield. ^{1}H NMR (CD_2Cl_2, 700 MHz): δ 10.14 (s, 1H, carbene), 8.52 (t, J = 7.8 Hz, 1H, pyr-*para* H), 8.03 (d, J = 7.8 Hz, 2H, pyr-*meta* H), 7.10 (t, J = 7.6 Hz, 1H, Xy-*para* H), 7.03 (s, 2H, MesDAP-*meta* H), 6.95 (d, J = 7.6 Hz, 2H, Xy-*meta* H), 6.90 (s, 2H, pyr-*meta* H), 6.08 (d, J = 20.8 Hz, 2H, pyr-CH_2-N), 5.49 (d, J = 20.8 Hz, 2H, pyr-CH_2-N), 3.58 (s, 3H, N-CH_3), 2.61 (s, 6H, MesDAP-CH_3), 2.35 (s, 6H, MesDAP-CH_3), 1.94 (s, 6H, MesDAP-CH_3), 1.28 (s, 6H, Xy-CH_3). ^{13}C NMR (CD_2Cl_2, 176 MHz): δ 241.89, 164.07, 156.40, 146.78, 145.01, 136.79, 135.45, 134.88, 132.71, 131.39, 130.39, 129.95, 128.94, 128.84, 127.87, 119.70, 75.72, 47.86, 20.43, 18.89, 17.66, 16.01. Anal. Calcd for $C_{36}H_{42}F_3N_4O_4ReS{\cdot}1/5CH_2Cl_2$: C, 49.02; N, 6.32; H, 4.82. Found: C, 49.12; N, 6.25; H, 4.96.

[(DAP)Re(O)(CHNCH$_3$(2,6-(CH$_3$)$_2$C$_6$H$_3$))][OTf] (DAP = 2,6-Bis-((arylamino)methyl)pyridine; Aryl = Xylyl; 8b). Complex **6a** (250. mg, 0.457 mmol) was dissolved in dichloromethane. 2,6-Dimethylphenyl isocyanide (120. mg, 0.914 mmol) was then added, and the reaction mixture was stirred for 5 min. Solvent was then removed in vacuo, and the resulting residue was washed with hexane, which was then removed via cannula filtration. The residue was then dissolved in dichoromethane, methyl trifluoromethanesulfonate (37.8 μL, 0.457 mmol) was added via syringe, and the reaction mixture was stirred for an additional 15 min. Solvent was then removed in vacuo, and the resulting residue was dissolved in minimal dichloromethane and precipitated with excess pentanes to give the complex in 35% yield. ^{1}H NMR (CD_2Cl_2, 700 MHz): δ 10.19 (s, 1H, carbene H), 8.52 (t, J = 7.8 Hz, 1H, pyr-*para* H), 8.01 (d, J = 7.9 Hz, 2H, pyr-*meta* H), 7.25−7.20 (m, 2H, XyDAP-*meta* H), 7.09 (d, J = 7.4 Hz, 2H, XyDAP-*meta* H), 7.08−7.02 (m, 3H, Xy-*para* and XyDAP-*para* H overlapping), 6.91 (d, J = 7.6 Hz, 2H, Xy-*meta* H), 6.10 (d, J = 20.8 Hz, 2H, pyr-CH_2-N), 5.50 (d, J = 20.8 Hz, 2H, pyr-CH_2-N), 3.59 (s, 3H, N-CH_3), 2.65 (s, 6H, XyDAP-CH_3), 1.97 (s, 6H, XyDAP-CH_3), 1.25 (s, 6H, Xy-CH_3). ^{13}C NMR (CD_2Cl_2, 176 MHz): δ 241.60, 164.02, 158.62, 146.68, 144.45, 135.83, 132.63, 131.80, 129.91, 129.52, 128.94, 128.84, 127.29, 119.05, 75.48, 47.91, 17.68, 17.62, 16.08. Anal. Calcd: C, 48.50; N, 6.65; H, 4.55. Found: C, 48.45; N, 6.64; H, 4.61.

(O)Re(DAP)(CHNH(2,6-(CH$_3$)$_2$C$_6$H$_3$))][HOB(C$_6$H$_5$)$_3$] (DAP = 2,6-Bis((arylamino)methyl)pyridine; Aryl = Mesityl; 10a). Complex **6a** (200. mg, 0.348 mmol) and $B(C_6F_5)_3$, (371. mg, 0.724 mmol) were dissolved in toluene. 2,6-Dimethylphenyl isocyanide (95.0 mg, 0.724 mmol) was then added, and the reaction mixture was stirred. The reaction mixture was then removed from the glovebox and stirred open to air until the color changed from green to dark purple and a solid precipitated (~15 min). The solid was then vacuum-filtered and washed with pentane to remove excess isocyanide. The complex was obtained as a light purple solid (237 mg) in 55% yield. ^{1}H NMR (CD_2Cl_2, 700 MHz): δ 13.21 (d, J = 16.0 Hz, 1H, N-H), 9.84 (d, J = 16.6 Hz, 1H, Carbene-H), 8.37 (t, J = 7.8 Hz, 1H, pyr-*para*-H), 7.88 (d, J = 7.8 Hz, 2H, pyr-*meta*-H), 6.94 (s, 2H, MesDAP-*meta*-H), 6.85 (t, J = 7.5 Hz, 1H, Xy-*para*-H), 6.77 (s, 2H, XyDAP-*meta*-H), 6.70 (d, J = 7.6 Hz, 2H, Xy-*meta*-H), 6.03 (d, J = 20.6 Hz, 2H, pyr-CH_2-N), 5.50 (d, J = 20.6 Hz, 2H, pyr-CH_2-N), 2.48 (s, 6H, MesDAP-CH_3), 2.23 (s, 6H, MesDAP-CH_3), 1.89 (s, 6H, MesDAP-CH_3), 1.35 (s, 6H, Xy-CH_3). ^{13}C NMR (CD2Cl2, 151 MHz) δ: 236.48, 164.69, 155.68, 143.45, 140.83, 136.37, 132.50, 130.52, 130.19, 129.21, 127.88, 127.22, 118.41, 75.32, 20.18, 17.55, 17.27, 16.15. ^{19}F NMR (CD_2Cl_2, 376 MHz): δ −137 (m, 2F, *meta*-F), −163 (m, 1F, *para*-F), −171 (m, 2F, *ortho*-F). Anal. Calcd: C, 50.54; N, 4.53; H, 3.34. Found: C, 50.18; N, 4.51; H, 3.38.

[(O)Re(DAP)(CHNH(2,6-(CH$_3$)$_2$C$_6$H$_3$))][HOB(C$_6$H$_5$)$_3$] (DAP = 2,6-Bis((arylamino)methyl)pyridine; Aryl = Xylyl; 10b). 6b (200. mg, 0.348 mmol) and $B(C_6F_5)_3$ (371 mg, 0.724 mmol) were dissolved in toluene. 2,6-Dimethylphenyl isocyanide (95.0 mg, 0.724 mmol) was then added, and the reaction mixture was stirred. The reaction mixture was then removed from the glovebox and stirred open to air until the color changed from green to dark purple and a solid precipitated (~15 min). The solid was then vacuum-filtered and washed with pentane to remove excess isocyanide. The complex was obtained as a light pink solid in 23% yield. ^{1}H NMR (CD_2Cl_2, 300 MHz): δ 13.49 (d, J = 16.4 Hz, 1H, NH), 9.89 (d, J = 16.4 Hz, 1H, Re-CH-N), 8.37 (t, J = 8.2 Hz, 1H, pyr-*para* H), 7.87 (d, J = 8.2 Hz, 2H, pyr-*meta* H), 7.1 (d, J = 7.0 Hz, 2H, XyDAP-*meta* H), 6.97−6.87 (m, 4H, overlapping XyDAP-*para* H and xylyl-*meta* H), 6.64 (d, J = 7.0 Hz, 2H, XyDAP-*meta* H), 6.02 (d, J = 19.9 Hz, 2H, pyr-CH_2-N), 5.50 (d, J = 19.9 Hz, 2H, pyr-CH_2-N), 2.50 (s, 6H, XyDAP-CH_3), 1.91 (s, 6H, XyDAP-CH_3), 1.30 (s, 6H, xylyl-CH_3). ^{19}F NMR (CD_2Cl_2, 376 MHz): δ −136 (m, 2F, *meta*-F), −162 (m, 1F, *para*-F), −166 (m, 2F, *ortho*-F). ^{13}C NMR (CD_2Cl_2, 151 MHz): δ 253.94, 164.60, 158.02, 136.83, 132.53, 129.66, 128.93, 128.12, 126.75, 118.50, 75.32, 21.12, 17.63, 17.41, 16.23. Anal. Calcd: C, 47.94; N, 4.41; H, 3.05. Found: C, 47.54; N, 4.83; H, 3.23.

[(O)Re(DAP)(CDNH(2,6-(CH$_3$)$_2$C$_6$H$_3$))][HOB(C$_6$H$_5$)$_3$] (DAP = 2,6-Bis((arylamino)methyl)pyridine; Aryl = Xylyl; 10b-D). The complex was obtained as a light pink solid in 21% yield. ^{1}H NMR (CD_2Cl_2, 300 MHz): δ 13.49 (s, 1H, NH), 8.37 (t, J = 8.2 Hz, 1H, pyr-*para* H), 7.87 (d, J = 8.2 Hz, 2H, pyr-*meta* H), 7.1 (d, J = 7.0 Hz, 2H, XyDAP-*meta* H), 6.97−6.87 (m, 4H, overlapping XyDAP-*para* H and xylyl-*meta* H), 6.64 (d, J = 7.0 Hz, 2H, XyDAP-*meta* H), 6.02 (d, J = 19.9 Hz, 2H, pyr-CH_2-N), 5.50 (d, J = 19.9 Hz, 2H, pyr-CH_2-N), 2.50 (s, 6H, XyDAP-CH_3), 1.91 (s, 6H, XyDAP-CH_3), 1.30 (s, 6H, xylyl-CH_3).

(O)Re(DAP)OH (DAP = 2,6-Bis((arylamino)methyl)pyridine; Aryl = Mesityl; 14). (O)Re(DAP)Cl (aryl = mesityl) (100 mg, 0.164 mmol) was placed in a screw-cap vial and dissolved in CD_3CN. $AgBF_4$ (32.1 mg, 0.164 mmol) was then added, and the solution was stirred at room temperature for 1 h. An 11.2 μL portion of 14.8 M NH_4OH was then added via microsyringe. The resulting mixture was then run through a Celite plug and analyzed by NMR spectroscopy. ^{1}H NMR (CD_2Cl_2, 600 MHz): δ 9.38 (s, 1H, Re-OH), 8.24 (t, J = 7.1 Hz, 1H, pyr-*para* H), 7.89 (d, J = 7.0 Hz, 2H, pyr-*meta* H), 6.97 (s, 2H, MesDAP-*meta* H), 6.89 (s, 2H, MesDAP-*meta* H), 5.68 (d, J = 20.7 Hz, 2H, pyr-CH_2-N), 5.51 (d, J = 20.7 Hz, 2H, pyr-CH_2-N), 2.49 (s, 6H, MesDAP-CH_3), 2.33 (s, 6H, MesDAP-CH_3), 1.64 (s, 6H, MesDAP-CH_3). ^{13}C NMR (CD_2Cl_2, 176 MHz): δ 167.80, 154.24, 143.35, 135.83, 134.69, 134.48, 128.58, 128.46, 117.10, 79.63, 20.58, 18.01, 17.86. Elemental analysis was not possible with this molecule because of its poor solubility in most solvents that are not halogenated. The compound reacts with halogenated solvents to generate the metal halide species.

Computational Methods. Theoretical calculations have been carried out using the Gaussian 09[31] implementation of B3PW91[25,26] density functional theory with the D3 version of Grimme's empirical dispersion correction.[26] All geometry optimizations were carried out in the gas phase using tight convergence criteria ("opt = tight") and pruned ultrafine grids ("Int = ultrafine"). The basis set for rhenium was the small-core (311111,22111,411) → [6s5p3d] Stuttgart−Dresden basis set and relativistic effective core potential (RECP) combination (SDD) with an additional f polarization function.[43−56] The 6-31G(d,p) basis set[57] was used for all other atoms. All structures were fully optimized. Analytical frequency calculations were performed on all structures to ensure either a zeroth-order saddle point (a local

DOI: 10.1021/acs.organomet.9b00600
Organometallics 2020, 39, 388−396

minimum) or a first-order saddle point (transition state: TS) was achieved. The minima associated with each transition state were determined by animation of the imaginary frequency.

Energetics were calculated on the gas-phase optimized structures as described above with the 6-311++G(d,p)[34] basis set for C, H, N, O, and F atoms and the SDD[43−55,58] basis set with an added f polarization function[56] on Re. Reported energies utilized analytical frequencies and the zero-point corrections from the gas-phase optimized geometries and included solvation corrections which were computed using the PCM method, with toluene as the solvent, as implemented in Gaussian 09. Mulliken population analysis (MPA) and charge decomposition analysis (CDA) were performed using AOMix 6.90.[29,30] Natural bond orbital (NBO) analysis was also conducted to obtain NBO atomic charges. This was performed with NBO 6.0.[27,28] Isotropic NMR shielding tensors were calculated using the SCF-GIAO method[36−40] 6-311++G(d,p)[34] basis set for C, H, N, O, and F atoms and the SDD basis set with an added f polarization function on Re. These values were then referenced to the isotropic NMR shielding tensors calculated for TMS (tetramethylsilane) using the 6-311++G(d,p)[34] basis set for C, H, and Si.

■ ASSOCIATED CONTENT

Supporting Information

The Supporting Information is available free of charge at https://pubs.acs.org/doi/10.1021/acs.organomet.9b00600.

Cartesian coordinates for the optimized geometries (XYZ)

Synthetic procedures, characterization data, and computational procedures (PDF)

Accession Codes

CCDC 1946750−1946754 contain the supplementary crystallographic data for this paper. These data can be obtained free of charge via www.ccdc.cam.ac.uk/data_request/cif, or by emailing data_request@ccdc.cam.ac.uk, or by contacting The Cambridge Crystallographic Data Centre, 12 Union Road, Cambridge CB2 1EZ, UK; fax: +44 1223 336033.

■ AUTHOR INFORMATION

Corresponding Author

*E-mail for E.A.I.: eaison@ncsu.edu.

ORCID

Elon A. Ison: 0000-0002-2902-2671

Author Contributions

The manuscript was written through contributions of all authors. All authors have given approval to the final version of the manuscript.

Notes

The authors declare no competing financial interest.

■ ACKNOWLEDGMENTS

We acknowledge North Carolina State University and the National Science Foundation via CHE-1664973 for funding. We also acknowledge the NCSU Office of Information Technology (OIT) High Performance Computing (HPC) for computational support.

■ REFERENCES

(1) de Frémont, P.; Marion, N.; Nolan, S. P. Carbenes: Synthesis, Properties, and Organometallic Chemistry. *Coord. Chem. Rev.* **2009**, *253*, 862−892.

(2) Brothers, P. J.; Roper, W. R. Transition-Metal Dihalocarbene Complexes. *Chem. Rev.* **1988**, *88*, 1293−1326.

(3) Won, J.; Jung, H.; Mane, M. V.; Heo, J.; Kwon, S.; Baik, M.-H. Schrock vs Fischer Carbenes: A Quantum Chemical Perspective. *Adv. Inorg. Chem.* **2019**, *73*, 385.

(4) Cross, J. L.; Crane, T. W.; White, P. S.; Templeton, J. L. Heteroatom-Substituted Carbene Complexes of High-Valent Tungsten: Tp'W(O)X(C(R)OSiR$_3$) Derivatives. *Organometallics* **2003**, *22*, 548−554.

(5) Malarek, M. S.; Evans, D. J.; Smith, P. D.; Bleeker, A. R.; White, J. M.; Young, C. G. Π-Acid/π-Base Carbonyloxomolybdenum (IV) Complexes and their Oxomolybdenum (VI/IV) Precursors. *Inorg. Chem.* **2006**, *45*, 2209−2216.

(6) Thomas, S.; Tiekink, E. R.; Young, C. G. Π-Acid/π-Base Carbonyloxo, Carbonylsulfido, and Mixed-Valence Complexes of Tungsten. *Inorg. Chem.* **2006**, *45*, 352−361.

(7) Lambic, N. S.; Lilly, C. P.; Robbins, L. K.; Sommer, R. D.; Ison, E. A. Reductive Carbonylation of Oxorhenium Hydrides Induced by Lewis Acids. *Organometallics* **2016**, *35*, 2822−2829.

(8) Lambic, N. S.; Lilly, C. P.; Sommer, R. D.; Ison, E. A. Mechanism for the Reaction of CO with Oxorhenium Hydrides: Migratory Insertion of CO into Rhenium Hydride and Formyl Bonds leads to Migration from Rhenium to the Oxo Ligand. *Organometallics* **2016**, *35*, 3060−3068.

(9) Smeltz, J. L.; Boyle, P. D.; Ison, E. A. Mechanism for the Activation of Carbon Monoxide via Oxorhenium Complexes. *J. Am. Chem. Soc.* **2011**, *133*, 13288−13291.

(10) Smeltz, J. L.; Boyle, P. D.; Ison, E. A. Role of Low-Valent Rhenium Species in Catalytic Hydrosilylation Reactions with Oxorhenium Catalysts. *Organometallics* **2012**, *31*, 5994−5997.

(11) Addison, A. W.; Rao, T. N.; Reedijk, J.; van Rijn, J.; Verschoor, G. C. Synthesis, Structure, and Spectroscopic Properties of Copper(II) Compounds containing Nitrogen−Sulphur Donor Ligands; the Crystal and Molecular Structure of Aqua[1,7-bis(N-methylbenzimidazol-2′-yl)-2,6-dithiaheptane]Copper(II) Perchlorate. *J. Chem. Soc., Dalton Trans.* **1984**, 1349−1356.

(12) Hahn, F. E.; Imhof, L. Reactions of 2-(Trimethylsiloxy)phenyl Isocyanide with Complexes of Rhenium in the + 1, + 3, and + 5 Oxidation States. *Organometallics* **1997**, *16*, 763−769.

(13) Schoultz, X.; Gerber, T. I. A.; Hosten, E. C. Formation of a Methine Carbon-to-Rhenium σ Bond in an Oxorhenium(V)-Benzothiazole Complex. *Inorg. Chem. Commun.* **2016**, *68*, 13−16.

(14) Smeltz, J. L.; Lilly, C. P.; Boyle, P. D.; Ison, E. A. The Electronic Nature of Terminal Oxo Ligands in Transition-Metal Complexes: Ambiphilic Reactivity of Oxorhenium Species. *J. Am. Chem. Soc.* **2013**, *135*, 9433−9441.

(15) Mayr, A.; Ahn, S. Oxidatively Induced Insertion of an Alkylidyne Unit into the Tungsten Tris(pyrazolyl)borate Cage. *Inorg. Chim. Acta* **2000**, *300−302*, 406−413.

(16) Oldham, J. W. J.; Oldham, S. M.; Scott, B. L.; Abney, K. D.; Smith, W. H.; Costa, D. A. Synthesis and Structure of -Heterocyclic Carbene Complexes of Uranyl Dichloride. *Chem. Commun.* **2001**, 1348−1349.

(17) Lilly, C. P.; Boyle, P. D.; Ison, E. A. Synthesis of Oxorhenium Acetyl and Benzoyl Complexes Incorporating Diamidopyridine Ligands: Implications for the Mechanism of CO Insertion. *Organometallics* **2012**, *31*, 4295−4301.

(18) Robbins, L. K.; Lilly, C. P.; Smeltz, J. L.; Boyle, P. D.; Ison, E. A. Synthesis and Reactivity of Oxorhenium(V) Methyl, Benzyl, and Phenyl Complexes with CO: Implications for a Unique Mechanism for Migratory Insertion. *Organometallics* **2015**, *34*, 3152−3158.

(19) Smeltz, J. L.; Webster, C. E.; Ison, E. A. Computational Investigation of the Mechanism for the Activation of CO by Oxorhenium Complexes. *Organometallics* **2012**, *31*, 4055−4062.

(20) Bergquist, C.; Bridgewater, B. M.; Harlan, C. J.; Norton, J. R.; Friesner, R. A.; Parkin, G. Aqua, Alcohol, and Acetonitrile Adducts of Tris(perfluorophenyl)borane: Evaluation of Brønsted Acidity and Ligand Lability with Experimental and Computational Methods. *J. Am. Chem. Soc.* **2000**, *122*, 10581−10590.

(21) Feng, Y.; Aponte, J.; Houseworth, P. J.; Boyle, P. D.; Ison, E. A. Synthesis of Oxorhenium(V) Complexes with Diamido Amine

DOI: 10.1021/acs.organomet.9b00600
Organometallics 2020, 39, 388−396

Ancillary Ligands and Their Role in Oxygen Atom Transfer Catalysis. *Inorg. Chem.* **2009**, *48*, 11058−11066.
(22) Lilly, C. P.; Boyle, P. D.; Ison, E. A. Synthesis and Characterization of Oxorhenium(v) Diamido Pyridine Complexes that Catalyze Oxygen Atom Transfer Reactions. *Dalton Trans.* **2011**, *40*, 11815−11821.
(23) Hartwig, J. F.; Collman, J. P. *Organotransition Metal Chemistry: from Bonding to Catalysis*; University Science Books: Sausalito, CA, 2010; Vol. *1*.
(24) Lambic, N. S.; Sommer, R. D.; Ison, E. A. Transition-Metal Oxos as the Lewis Basic Component of Frustrated Lewis Pairs. *J. Am. Chem. Soc.* **2016**, *138*, 4832−4842.
(25) Becke, A. D. Density-Functional Exchange-Energy Approximation with Correct Exchange. *J. Chem. Phys.* **1993**, *98*, 5648−5652.
(26) Grimme, S.; Antony, J.; Ehrlich, S.; Krieg, H. A Consistent and Accurate Ab Initio Parametrization of Density Functional Dispersion Correction (DFT-D) for the 94 Elements H-Pu. *J. Chem. Phys.* **2010**, *132*, 154104.
(27) Foster, J.; Weinhold, F. Natural Hybrid Orbitals. *J. Am. Chem. Soc.* **1980**, *102*, 7211−7218.
(28) Weinhold, F.; Glendening, E. D. *NBO 5.0 program Manual: Natural Bond Orbital Analysis Programs*; Theoretical Chemistry Institute and Department of Chemistry, University of Wisconsin: Madison, WI, 2001.
(29) Gorelsky, S. *AOMix Program for Molecular Orbital Analysis-Version 6.5*; University of Ottawa: Ottawa, Canada, 2011; http://www.sg-chem.net.
(30) Gorelsky, S.; Lever, A. Electronic Structure and Spectra of Ruthenium Diimine Complexes by Density Functional Theory and INDO/S. Comparison of the Two Methods. *J. Organomet. Chem.* **2001**, *635*, 187−196.
(31) Frisch, M.; Trucks, G.; Schlegel, H.; Scuseria, G.; Robb, M.; Cheeseman, J.; Scalmani, G.; Barone, V.; Mennucci, B.; Petersson, G., et al. *Gaussian 09*; Gaussian. Inc.: Wallingford, CT, 2009.
(32) Kreiter, C. G.; Formáček, V. Unusual ^{13}C Chemical Shifts of Transition Metal-Carbene Complexes. *Angew. Chem., Int. Ed. Engl.* **1972**, *11*, 141−142.
(33) Ciappenelli, D. J.; Cotton, F. A.; Kruczynski, L. Carbon-13 NMR Spectra of Chromium Pentacarbonyl Carbenoid Complexes. *J. Organomet. Chem.* **1973**, *50*, 171−174.
(34) Krishnan, R.; Binkley, J. S.; Seeger, R.; Pople, J. A. Self-Consistent Molecular Orbital Methods. XX. A Basis Set for Correlated Wave Functions. *J. Chem. Phys.* **1980**, *72*, 650−654.
(35) Clark, T.; Chandrasekhar, J.; Spitznagel, G. W.; Schleyer, P. V. R. Efficient Diffuse Function-Augmented Basis Sets for Anion Calculations. III. The 3-21+ G Basis Set for First-Row Elements, Li−F. *J. Comput. Chem.* **1983**, *4*, 294−301.
(36) London, F. Théorie Quantique des Courants Interatomiques dans les Combinaisons Aromatiques. *J. Phys. Radium* **1937**, *8*, 397−409.
(37) McWeeny, R. Perturbation Theory for the Fock-Dirac Density Matrix. *Phys. Rev.* **1962**, *126*, 1028−1034.
(38) Ditchfield, R. Self-Consistent Perturbation Theory of Diamagnetism. *Mol. Phys.* **1974**, *27*, 789−807.
(39) Wolinski, K.; Hinton, J. F.; Pulay, P. Efficient Implementation of the Gauge-Independent Atomic Orbital Method for NMR Chemical Shift Calculations. *J. Am. Chem. Soc.* **1990**, *112*, 8251−8260.
(40) Cheeseman, J. R.; Trucks, G. W.; Keith, T. A.; Frisch, M. J. A Comparison of Models for Calculating Nuclear Magnetic Resonance Shielding Tensors. *J. Chem. Phys.* **1996**, *104*, 5497−5509.
(41) Guérin, F.; McConville, D. H.; Vittal, J. J. Conformationally Rigid Diamide Complexes of Zirconium: Electron Deficient Analogues of Cp_2Zr. *Organometallics* **1996**, *15*, 5586−5590.
(42) Bryan, J. C.; Stenkamp, R. E.; Tulip, T. H.; Mayer, J. M. Oxygen Atom Transfer among Rhenium, Sulfur, and Phosphorus. Characterization and Reactivity of $Re(O)Cl_3(Me_2S)(OPPh_3)$ and $Re(O)Cl_3(CNCMe_3)_2$. *Inorg. Chem.* **1987**, *26*, 2283−2288.
(43) Cao, X.; Dolg, M. Valence Basis Sets for Relativistic Energy-Consistent Small-Core Lanthanide Pseudopotentials. *J. Chem. Phys.* **2001**, *115*, 7348−7355.
(44) Cao, X.; Dolg, M. Segmented Contraction Scheme for Small-Core Lanthanide Pseudopotential Basis Sets. *J. Mol. Struct.: THEOCHEM* **2002**, *581*, 139−147.
(45) Leininger, T.; Nicklass, A.; Stoll, H.; Dolg, M.; Schwerdtfeger, P. The Accuracy of the Pseudopotential Approximation. II. A Comparison of Various Core Sizes for Indium Pseudopotentials in Calculations for Spectroscopic Constants of InH, InF, and InCl. *J. Chem. Phys.* **1996**, *105*, 1052−1059.
(46) Nicklass, A.; Dolg, M.; Stoll, H.; Preuss, H. Ab Initio Energy-Adjusted Pseudopotentials for the Noble Gases Ne through Xe: Calculation of Atomic Dipole and Quadrupole Polarizabilities. *J. Chem. Phys.* **1995**, *102*, 8942−8952.
(47) Küchle, W.; Dolg, M.; Stoll, H.; Preuss, H. Energy-Adjusted Pseudopotentials for the Actinides. Parameter Sets and Test Calculations for Thorium and Thorium Monoxide. *J. Chem. Phys.* **1994**, *100*, 7535−7542.
(48) Dolg, M.; Stoll, H.; Preuss, H.; Pitzer, R. M. Relativistic and Correlation Effects for Element 105 (hahnium, Ha): a Comparative Study of M and MO (M = Nb, Ta, Ha) using Energy-Adjusted Ab Initio Pseudopotentials. *J. Phys. Chem.* **1993**, *97*, 5852−5859.
(49) Häussermann, U.; Dolg, M.; Stoll, H.; Preuss, H.; Schwerdtfeger, P.; Pitzer, R. M. Accuracy of Energy-Adjusted Quasirelativistic Ab Initio Pseudopotentials. *Mol. Phys.* **1993**, *78*, 1211−1224.
(50) Fuentealba, P.; Szentpaly, L. v.; Preuss, H.; Stoll, H. Pseudopotential Calculations for Alkaline-Earth Atoms. *J. Phys. B: At. Mol. Phys.* **1985**, *18*, 1287−1296.
(51) Stoll, H.; Fuentealba, P.; Schwerdtfeger, P.; Flad, J.; Szentpály, L. v.; Preuss, H. Cu and Ag as One-Valence-Electron Atoms: CI Results and Quadrupole Corrections for Cu_2, Ag_2, CuH, and AgH. *J. Chem. Phys.* **1984**, *81*, 2732−2736.
(52) Fuentealba, P.; Stoll, H.; Szentpaly, L. v.; Schwerdtfeger, P.; Preuss, H. On the Reliability of Semi-Empirical Pseudopotentials: Simulation of Hartree-Fock and Dirac-Fock Results. *J. Phys. B: At. Mol. Phys.* **1983**, *16*, L323−L328.
(53) von Szentpály, L.; Fuentealba, P.; Preuss, H.; Stoll, H. Pseudopotential Calculations on Rb^+_2, Cs^+_2, RbH^+, CsH^+ and the Mixed Alkali Dimer Ions. *Chem. Phys. Lett.* **1982**, *93*, 555−559.
(54) Fuentealba, P.; Preuss, H.; Stoll, H.; Von Szentpály, L. A Proper Account of Core-Polarization with Pseudopotentials: Single Valence-Electron Alkali Compounds. *Chem. Phys. Lett.* **1982**, *89*, 418−422.
(55) Dunning, T. H.; Hay, P. J., Methods of Electronic Structure Theory. In *Modern Theoretical Chemistry*; Plenum Press: New York, 1977; Vol. *3*, p 1.
(56) Ehlers, A.; Böhme, M.; Dapprich, S.; Gobbi, A.; Höllwarth, A.; Jonas, V.; Köhler, K.; Stegmann, R.; Veldkamp, A.; Frenking, G. A Set of f-Polarization Functions for Pseudo-Potential Basis Sets of the Transition Metals Sc−Cu, Y−Ag and La−Au. *Chem. Phys. Lett.* **1993**, *208*, 111−114.
(57) Hehre, W. J.; Ditchfield, R.; Pople, J. A. Self—Consistent Molecular Orbital Methods. XII. Further Extensions of Gaussian—Type Basis Sets for use in Molecular Orbital Studies of Organic Molecules. *J. Chem. Phys.* **1972**, *56*, 2257−2261.
(58) Bergner, A.; Dolg, M.; Küchle, W.; Stoll, H.; Preuß, H. Ab Initio Energy-Adjusted Pseudopotentials for Elements of Groups 13−17. *Mol. Phys.* **1993**, *80*, 1431−1441.

DOI: 10.1021/acs.organomet.9b00600
Organometallics 2020, 39, 388−396